International Journal of ChemTech Research
CODEN (USA): IJCRGG ISSN: 0974-4290
Vol.8, No.11 pp 443-449, 2015

Degradation of Textile Effluent using Nanocomposite TiO_2/SnO_2 Semiconductor Photocatalysts

N. Karthikeyan[1], V. Narayanan[2] and A. Stephen[1]

[1]Department of Nuclear Physics, University of Madras, Guindy Campus, Chennai, India
[2]Department of Inorganic Chemistry, University of Madras, Guindy Campus, Chennai, India

Abstract: TiO_2, SnO_2 semiconductor nanomaterials and TiO_2/SnO_2 semiconductor nanocomposites with the weight percentages of 97:3, 95:5 and 90:10 were prepared. These as prepared materials were annealed at the optimized temperature of 450 ^{0}C for 2 hours. The crystalline structures of the prepared nanomaterials were confirmed by XRD and the surface morphology of the samples was studied by FESEM and TEM. The average crystallite sizes of the spherically shaped particles were found to be in the range from 4 nm to 11 nm. The elemental compositions of the catalysts were confirmed by EDX. The optical properties of the powder samples were analyzed with UV-VIS spectroscopy and their band gaps were estimated. Degradation abilities of the synthesized nanophotocatalysts on methylene blue and textile effluent collected from textile industries in Tiruppur, India were tested. The TiO_2/SnO_2 (95:5) nanocomposite showed the best degradation efficiency.
Keywords: Semiconductor photocatalysts, Titania, Tin oxide, Nanocomposite.

Introduction

TiO_2 photocatalysis has its origins in early research effort into photoelectrochemical systems for solar to chemical energy conversion. In 1972, Fujishima and Honda in their landmark study found that TiO_2 could be used as catalytic electrode in photoelectrolysis cell to decompose water into H_2 and O_2, without applying an external voltage [1]. After a few years it was realized that this Fujishima-Honda microcells, consisting TiO_2 particles with deposit of Pt on them, was also able to work as photocatalysts for splitting H_2O. Since then, much active attention was given to the use of TiO_2 for photo-assisted degradation of organic compounds and reduction of inorganic compounds [2-8].

As a semiconductor oxide with wide-band gap in the order of 3.0 - 3.2 eV, TiO_2 is easy to be irradiated especially by UV light to create the excited electron–hole pairs which could separate and the resulting charge carriers might migrate to the surface where they react with adsorbed water and oxygen to produce radical species. These radicals strike any adsorbed organic molecules, resulting in complete or selective decomposition. Several studies have been reported on the photocatalytic degradation of textile dyes by TiO_2. The efficient photo generation of electron-hole pairs and the prevention of recombination of them are two key factors in increasing the efficiency of photocatalytic activity [9-11]. Several researches proved that the recombination is prevented by semiconductor-metal composites or by employing two different semiconductors [2, 12-15]. When a composite is prepared with a wider band gap semiconductor, which has more positive conduction band edge than that of the smaller band gap semiconductor, then the electrons from smaller band gap semiconductor can be injected into the larger band gap semi-conductor, that coupling can effectively prevent the recombination [16, 17].

In this study, TiO_2, SnO_2 and coupled TiO_2/SnO_2 photocatalysts at different weight percentages were prepared by multiple stage chemical methods at the optimized annealing temperature of 450 ^{0}C for TiO_2 [18] and the prepared semiconductor photocatalysts were first employed in degrading a model textile dye, methylene blue (MB), and then the identified best semiconductor photocatalyst was employed in degrading the textile effluent.

Experimental

Preparation of materials

TiO_2 was synthesized through the sol-gel method by dissolving the precursor titanium isopropoxide in isopropanol under continuous stirring at room temperature, and then adding citric acid as the chelating agent mixed with distilled water. SnO_2 was prepared through precipitation route by dissolving the precursor $SnCl_4.5H_2O$ in double distilled water under continuous stirring at room temperature, and then adding NaOH solution. The precipitate was washed, filtered and dried under similar experimental conditions. The dried samples were annealed at the optimized temperature 450 ^{o}C for 2 hours [18]. TiO_2/SnO_2 nanocomposites were prepared in three different weight percentage compositions of 97:03, 95:05 and 90:10. The respective compositions were ground for 2 hours and then sintered at 450 ^{0}C for 2 hours. The model dye solution was prepared by dissolving 9.8 mg of MB in 1000 ml of distilled water. The textile effluent was diluted to meet optimal experimental conditions.

Characterisation of materials

Crystalline structures of the annealed samples were determined by the powder XRD RICH SEIFERT diffractometer using Cu $K_{\alpha 1}$ radiation (λ = 0.154056 nm). The averaged crystallite sizes were estimated using the Scherrer's formula. Surface morphology and elemental analysis were carried out using FESEM and EDX. Particle size distributions were probed by TEM. The light absorption property of the samples and the degradations of methylene blue dye and textile effluents were studied with UV-VIS spectrophotometer.

Photocatalytic degradation experiment

The photocatalytic degradation activity was studied with an indigenously designed reaction chamber fitted with an 8W mercury vapour UV light source and a magnetic stirrer was setup inside a dark enclosure. Reaction suspensions were prepared by adding required amount of synthesized photocatalysts into 100 ml of MB solution, under continuous stirring. Then photocatalytic decomposition study of MB was carried out under UV light irradiation. The samples from the suspensions were collected at equal intervals of time, centrifuged and filtered. The decolouration of methylene blue was analysed by UV-Vis spectrophotometer at the wavelength of 664 nm. Decolourization was estimated using the formula, C_t/C_0, where C_0 is the initial concentration and C_t is the concentration of irradiated suspension at time t, taken at regular intervals. The best photocatalyst was then employed to degrade textile effluent collected from textile industries in Tiruppur, Tamil Nadu, India, under similar conditions.

Results and Discussion

XRD analysis

The XRD patterns of the prepared TiO_2 and SnO_2 samples are shown in figure 1. The characteristic peaks of anatase phase TiO_2 exhibit tetragonal structure and matches with the JCPDS number 78-2486, with its lattice parameters, a = b = 3.784 Å and c = 9.561 Å. And that of SnO_2 exhibit tetragonal structure and matches with the JCPDS number 41-1445, with its lattice parameters, a = b = 4.753 Å and c = 3.184 Å. The estimated mean crystallite size for TiO_2 was approximately 5 nm and that for SnO_2 was approximately 4 nm.

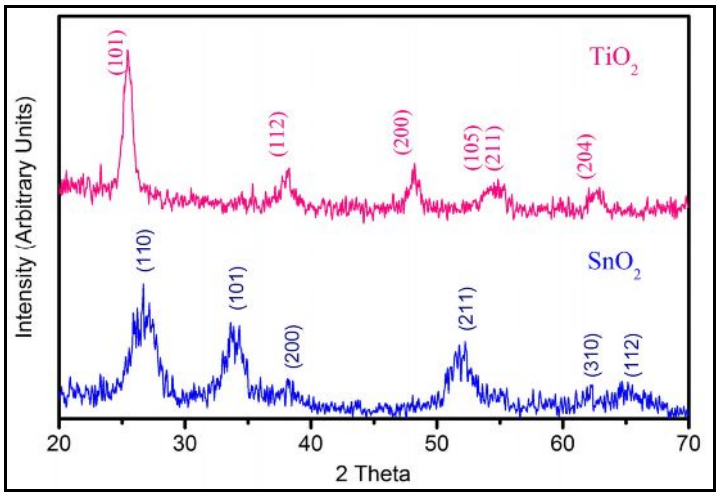

Figure 1: XRD spectra of TiO_2 and SnO_2 annealed at 450 ^{0}C

The figure 2 shows the XRD patterns of TiO_2/SnO_2 nanocomposites prepared at different weight percentages of 97:03, 95:05, and 90:10. Slight increase in peak intensities of anatase TiO_2 were observed with higher percentages of SnO_2 and the weight percentage 95:05 showed the highest increase in the peak intensities. No significant peak shifts were observed in all the three XRD patterns. The mean crystallite sizes were estimated to be from 9 nm to 11 nm.

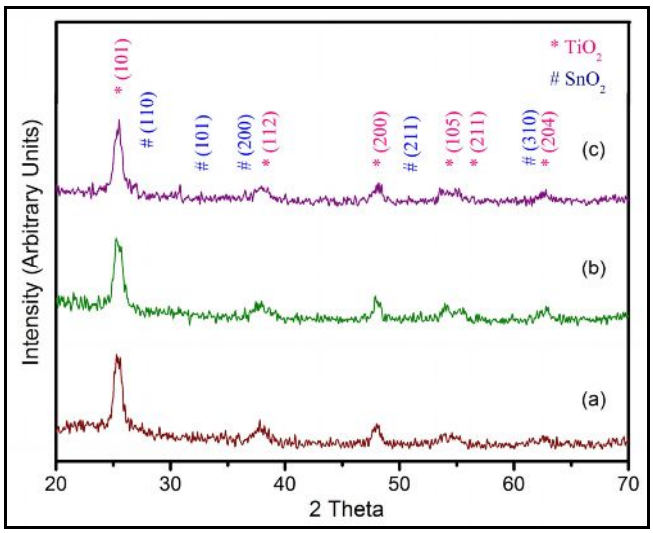

Figure 2: XRD spectra of TiO_2 /SnO_2 (a) 97:03, (b) 95:05 and (c) 90:10

FESEM and EDX analysis

Figure 3(a) shows the FESEM images for TiO_2/SnO_2 (95:05) nanocomposite annealed at 450 ^{0}C for 2 h. These images reveal irregular shaped particles which are the agglomeration of tiny spherically shaped crystals. The average particle sizes of the isolated spheres in the images shown in figure 3(b) are in the range from 9 nm to 13 nm.

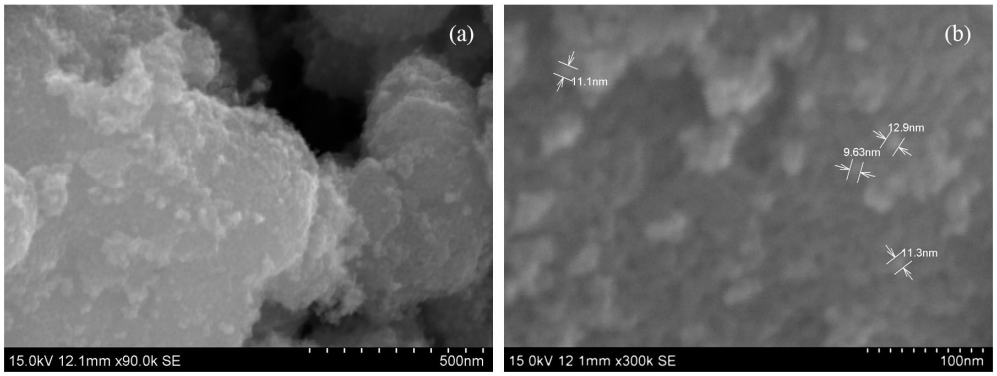

Figure 3: FESEM images of TiO_2/SnO_2 (95:05) annealed at 450 ^{0}C

EDX spectrum for TiO_2/SnO_2 (95:05) nanocomposite is shown in figure 4, which establish the presence of respective elements without any impurities. Presence of carbon was due to the usage of carbon substrate as sample holder.

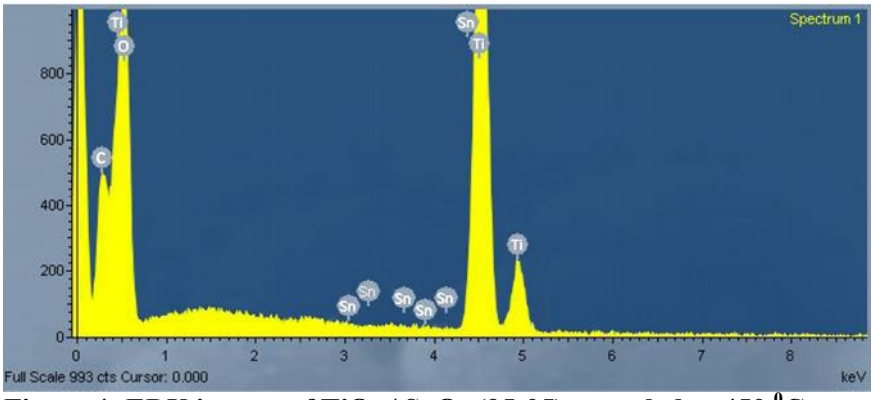

Figure 4: EDX images of TiO_2 / SnO_2 (95:05) annealed at 450 ^{0}C

TEM analysis

TEM images taken to determine the shape, size and size distribution of nanoparticles and the particle distribution plot are shown in figure 5. These results are in agreement with the results obtained from the XRD and the SEM investigations.

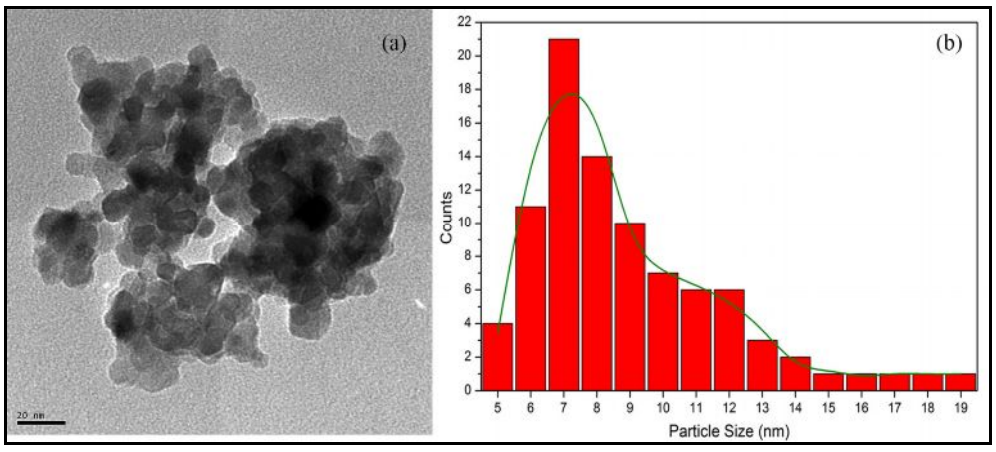

Figure 5: (a) TEM image and (b) particle size distribution of TiO_2/SnO_2 (95:05) photocatalyst

Optical properties of the photocatalysts

The optical properties of the prepared samples were studied with UV-Vis Diffused Reflectance Spectroscopy (DRS) and the results are depicted in the figure 6.

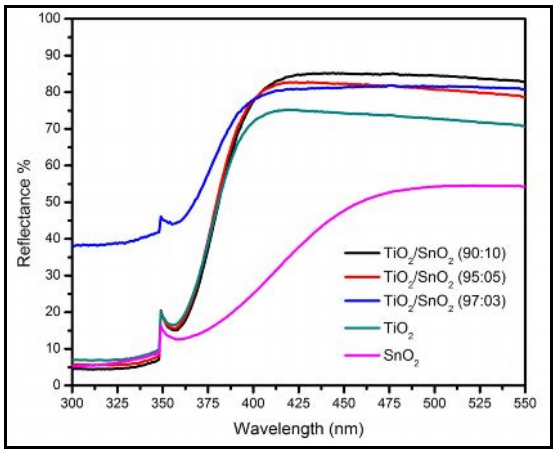

Figure 6: UV-Vis spectra of the prepared samples

The UV-Vis DRS spectrum of TiO_2, SnO_2, TiO_2/SnO_2 (97:03), TiO_2/SnO_2 (95:05), and TiO_2/SnO_2 (90:10) shows absorption edges in the UV region and these properties suggest photocatalytic activity under UV light irradiation. The estimated band gap energies for TiO_2, SnO_2, TiO_2/SnO_2 (97:3), TiO_2/SnO_2 (95:5), and TiO_2/SnO_2 (90:10) were 3.18 eV, 3.78 eV, 3.15 eV, 3.08 eV and 3.00 eV respectively.

The degradation profile of MB and Textile Effluent

The degradation profile of methylene blue by all the prepared samples under UV light irradiation is shown in figure 7(a). The highest photocatalytic degradation of about 90% was achieved by the nanocomposite TiO_2/SnO_2 (95:05) in 2 hrs. However, lower photocatalytic activity was observed for the TiO_2/SnO_2 (90:10) nanocomposite composition, though its band gap was less than that of (95:05) composition. It may be due to deposition of excess SnO_2 on the surfaces at higher composition of SnO_2 over a critical value, and thus reduces the photocatalytic activity. The pure SnO_2 showed very little photocatalytic activity under irradiation of UV light.

Then the best photocatalyst and Titania were employed to degrade the textile effluent. Titania was employed for comparison purposes. The degradation profile shown in figure 7(b) indicates about 60% of degradation in 5 hours by TiO_2/SnO_2 (95:05) which is a significant performance compared to that of pure Titania in the same duration. The results in both cases indicate improvement of photocatalytic degradation by the nanocomposite TiO_2/SnO_2 semiconductor photocatalysts compared to that by the pure TiO_2. Enhanced degradation process will be discussed later in detail in the proposed degradation mechanism.

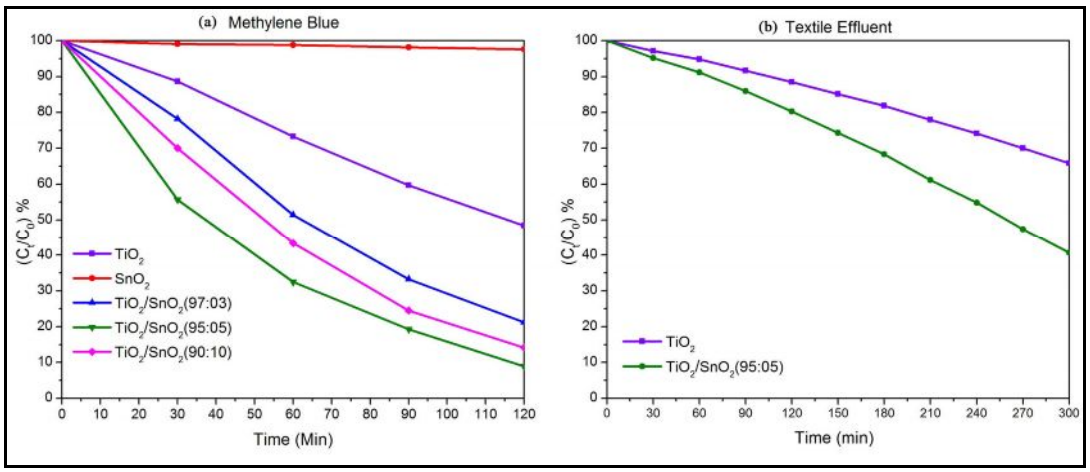

Figure 7: Degradation profile of (a) methylene blue and (b) textile effluent

Proposed Photocatalytic Mechanism:

Energy band diagram in figure 8(a) shows the relative positions of conduction bands and valence bands of SnO_2 and TiO_2. The proposed photocatalytic mechanism for the prepared composite TiO_2/SnO_2 photocatalysts is shown in figure 8(b). Under the UV light irradiation, electrons in TiO_2 are excited to its conduction band. When two semiconductors are closely coupled in the nanocomposite, conduction and valence bands of SnO_2 act as sink for the photogenerated electrons. This minimizes the recombination of the photo-generated electron-hole pairs in TiO_2 and gives sufficient time for these electrons and holes to migrate across the surface of the coupled nanocomposite photocatalysts where these pairs participate in redox reactions with the MB or textile effluent that are adsorbed to the surfaces of the photocatalysts. The holes can react with surface-bond H_2O (or) OH^- to produce the hydroxyl radical and the electrons can reduce surface adsorbed O_2 to generate superoxide radical ions (O_2^-). The mechanism is as follows:

$$TiO_2 \xrightarrow{h\nu} e^- + h^+$$

(1) $h^+ + OH^- \rightarrow OH^\bullet$ (Oxidation)

$h^+ + H_2O \rightarrow OH^\bullet + H^+$

(2) $O_2 + e^- \rightarrow {}^\bullet O_2^-$ (Reduction)

${}^\bullet O_2^- + H^+ \rightarrow HO_2^\bullet$

$O_2^\bullet + HO_2^\bullet \rightarrow H_2O_2 + O_2$

${}^\bullet O_2^- + HO_2^\bullet \rightarrow HO_2^- + O_2$

$HO_2^- + H^+ \rightarrow H_2O_2$

(3) $H_2O_2 + {}^\bullet O_2^- \rightarrow OH^\bullet + OH^\bullet + O_2$

$H_2O_2 + e^- \rightarrow OH^\bullet + OH^-$

$OH^\bullet$ + MB or Textile Effluent $\rightarrow$ Products

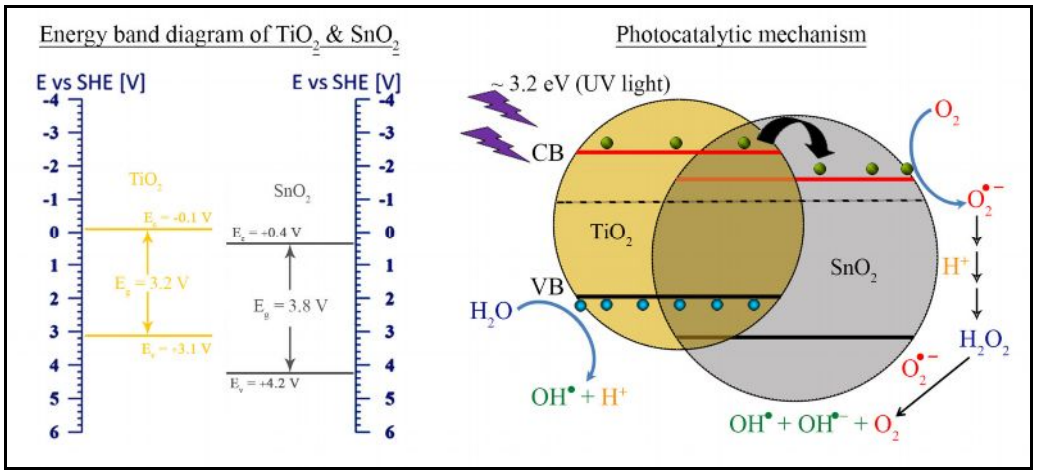

Figure 8: Energy band diagram and Photocatalytic degradation mechanism

Conclusions

The TiO_2 and SnO_2 nanopowders and coupled TiO_2/SnO_2 nanophotocatalysts with different weight percentages were synthesized. The mean crystallite sizes of irregular spherically shaped nanoparticles were found to be in the range from 4 nm to 13 nm and particle sizes of the best photocatalyst TiO_2/SnO_2 (90:05) were found to be in the range from 5 nm to 19 nm. The bandgap energies were deduced from the optical analysis and the bandgap of TiO_2/SnO_2 nanocomposite was found to be decreasing with increasing weight percentage of SnO_2.

The degradation abilities of the prepared photocatalysts on methylene blue dye and textile dye effluent were tested with irradiation of UV light. The TiO_2/SnO_2 nanocomposites showed considerable enhancement of photocatalytic degradation activities than the pure TiO_2 in both cases. The pure SnO_2 showed negligible photocatalytic degradation. The TiO_2/SnO_2 (95:05) nanocomposite showed the best photocatalytic degradation activity. The enhancement in photocatalytic activities could be attributed to reduced band gap, reduction of

recombination, and efficient migration of the charge carriers due to effectively coupled TiO_2/SnO_2 in nanocomposite form, and enhanced adsorption methylene blue or textile effluent molecules to the photocatalysts having larger specific surface area due to spherically shaped smaller sizes of the photocatalyst particles.

Acknowledgements

Authors are thankful to National Centre for Nanoscience and Nanotechnology, University of Madras for FESEM, EDX and TEM characterisation. One of the authors, NK, thanks HETC project for the financial support.

References

1. Fujishima, A. and K. Honda, *Electrochemical Photolysis of Water at a Semiconductor Electrode.* Nature, 1972. 238(5358): p. 37-38.
2. Vaezi, M.R., *Two-step solochemical synthesis of ZnO/TiO2 nano-composite materials.* Journal of Materials Processing Technology, 2008. 205(1-3): p. 332-337.
3. Kumar, S.G. and L.G. Devi, *Review on Modified TiO2 Photocatalysis under UV/Visible Light: Selected Results and Related Mechanisms on Interfacial Charge Carrier Transfer Dynamics.* The Journal of Physical Chemistry A, 2011. 115(46): p. 13211-13241.
4. Huber, D.L. and T.C. Monson, *High-yield synthesis of Brookite TiO2 Nanoparticles*, U.S. Patent, Editor 2011, Sandia Corporation, Albuquerque, NM (US): US. p. 6.
5. Choi, J. and K. Park, *Effect of reaction atmosphere on particle morphology of TiO2 produced by thermal decomposition of titanium tetraisopropoxide.* Journal of Nanoparticle Research, 2006. 8(2): p. 269-278.
6. Pfleiderer, S.J., D. Lützenkirchen-Hecht, and R. Frahm, *Crystallization behaviour of TiO2–ZrO2 composite nanoparticles.* Journal of Sol-Gel Science and Technology, 2012. 64(1): p. 27-35.
7. Hernandez-Alonso, M.D., et al., *Development of alternative photocatalysts to TiO2: Challenges and opportunities.* Energy & Environmental Science, 2009. 2(12): p. 1231-1257.
8. Shankar, H., et al., *Synthesis, characterization and photocatalytic activity of nanotitania loaded W-MCM-41.* Nanotechnology, 2008. 19(31): p. 315711.
9. Michael A, H., *A surface science perspective on photocatalysis.* Surface Science Reports, 2011. 66(6-7): p. 185-297.
10. Fujishima, A., X. Zhang, and D.A. Tryk, *TiO2 photocatalysis and related surface phenomena.* Surface Science Reports, 2008. 63(12): p. 515-582.
11. Fox, M.A. and M.T. Dulay, *Heterogeneous photocatalysis.* Chemical Reviews, 1993. 93(1): p. 341-357.
12. Jakob, M., H. Levanon, and P.V. Kamat, *Charge Distribution between UV-Irradiated TiO2 and Gold Nanoparticles: Determination of Shift in the Fermi Level.* Nano Letters, 2003. 3(3): p. 353-358.
13. Ni, M., et al., *A review and recent developments in photocatalytic water-splitting using for hydrogen production.* Renewable and Sustainable Energy Reviews, 2007. 11(3): p. 401-425.
14. Wood, A., M. Giersig, and P. Mulvaney, *Fermi Level Equilibration in Quantum Dot−Metal Nanojunctions†.* The Journal of Physical Chemistry B, 2001. 105(37): p. 8810-8815.
15. Saravanan, R., et al., *Photocatalytic Degradation of Organic Dyes Using ZnO/CeO_2 Nanocomposite Material Under Visible Light.* Advanced Materials Research, 2012. 584(1): p. 381-385.
16. Yang, S., et al., *Ultrathin SnO2 Scaffolds for TiO2-Based Heterojunction Photoanodes in Dye-Sensitized Solar Cells: Oriented Charge Transport and Improved Light Scattering.* Chemistry – A European Journal, 2013. 19(28): p. 9366-9370.
17. Tiwana, P., et al., *Electron Mobility and Injection Dynamics in Mesoporous ZnO, SnO2, and TiO2 Films Used in Dye-Sensitized Solar Cells.* ACS Nano, 2011. 5(6): p. 5158-5166.
18. Karthikeyan, N., R. Saravanan, and A. Stephen, *Photocatalytic applications of nano-titania phases.* 3rd International Conference on Advances in Materials and Materials Processing, 2011. 3(1): p. 188.

*****